

Pilot-Scale Studies of Process Intensification by Cyclic Distillation

Bogdan V. Maleta

Maleta Cyclic Distillation LLC OÜ, Tallinn 11317, Estonia

Alexander Shevchenko and Olesja Bedryk

National University of Food Technologies, Department of Processes and Apparatus for Food Production, Kyiv 01601, Ukraine

Anton A. Kiss

AkzoNobel - Research, Development & Innovation, Process Technology SRG, Deventer 7418 AJ, The Netherlands

University of Twente, Faculty of Science and Technology, Sustainable Process Technology Group, Enschede 7500 AE, The Netherlands

DOI 10.1002/aic.14827

Published online April 20, 2015 in Wiley Online Library (wileyonlinelibrary.com)

Process intensification in distillation systems receives much attention with the aim of increasing both energy and separation efficiency. Several technologies have been investigated and developed, as for example: dividing-wall column, HiGee distillation, or internal heat-integrated distillation. Cyclic distillation is a different method based on separate phase movement—achievable with specific internals and a periodic operation mode—that leads to key advantages: increased column throughput, reduced energy requirements, and better separation performance. This article is the first to report the performance of a pilot-scale distillation column for ethanol-water separation, operated in a cyclic mode. A comparative study is made between a pilot-scale cyclic distillation column and an existing industrial beer column used to concentrate ethanol. Using specially designed trays that truly allow separate phase movement, the practical operation confirmed that 2.6 times fewer trays and energy savings of about 30% are possible as compared with classic distillation.

© 2015 American Institute of Chemical Engineers *AIChE J.*, 61: 2581–2591, 2015

Keywords: cyclic distillation, process intensification, mass transfer, efficiency, energy savings, beer column

Introduction

Advanced distillation technologies were developed with the main aim of increasing both energy and separation efficiency, as for example: dividing-wall column, HiGee distillation, internal heat-integrated distillation, membrane distillation, cyclic distillation, and reactive distillation.^{1,2} Most of these process intensification techniques use the continuous counter-current contact of vapor and liquid phases, except for cyclic distillation that uses an alternative operating mode based on separate phase movement. Cyclic distillation could be easily implemented in existing columns by simply changing the internals and the operating mode, thus bringing new life in old towers by significantly increasing the column throughput, reducing the energy requirements, and offering a better separation performance.^{3,4}

References to periodic operation of distillation go back to the early 60s when the idea of cyclic operation in distillation, liquid–liquid extraction, and particle separation was first introduced.⁵ In case of cyclic distillation, one operating cycle

consists of two parts: a vapor-flow period, when the thrust of the rising vapor prevents liquid downflow (e.g., vapor velocity exceeds the weeping limit), followed by a liquid-flow period when the liquid flows down the column, dropping by gravity, first to the sluice chamber and then moving from each tray to the tray below—as shown in Figure 1.⁴ With this type of operation, no downcomers are needed hence, the plates are simple, inexpensive, and flexible.⁶ The time for each period is imposed using a timer that controls the valve in the vapor line connecting the reboiler to the distillation tower. Improved separation performance is possible as a result of separate phase movement and lack of mixing between the liquid from different trays (which have different composition). Remarkable, the concept of cyclic distillation could be further extended to catalytic cyclic distillation, a novel setup that can efficiently combine the benefits of reactive distillation with the ones of cyclic operation mode.⁷

The cyclic mode of operation was experimentally tested using conventional internals, for several separations such as: benzene/toluene (brass and mesh-screen plates),⁸ methylcyclohexane/n-heptane (packed plates),⁹ acetone/water (sieve trays),¹⁰ and methanol/water.^{11,12} These early results proved key benefits of the cyclic operation mode as compared with conventional distillation: higher capacity and higher tray

Correspondence concerning this article should be addressed to A. A. Kiss at Tony.Kiss@akzonobel.com or TonyKiss@gmail.com.

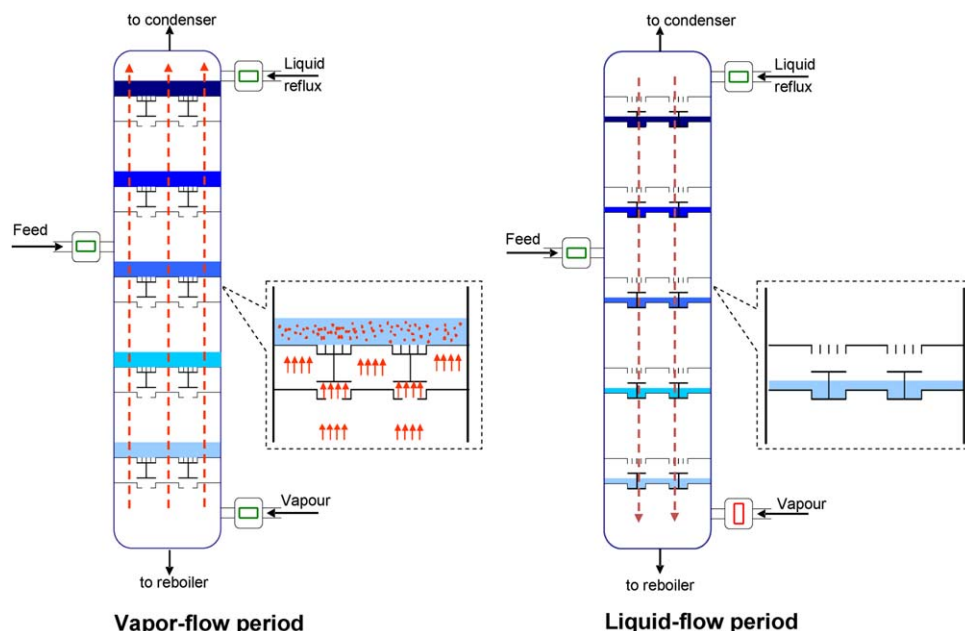


Figure 1. Cyclic distillation works by alternating a vapor-flow period (left) with a liquid-flow period (right).

[Color figure can be viewed in the online issue, which is available at wileyonlinelibrary.com.]

efficiency. Therefore, larger feed rates can be processed and the required separation can be achieved using lower energy input (at the same number of trays) or fewer trays (at the same energy input). The experimental results also proved the hydrodynamics limitations of the cyclic operation mode, as separate movement of the liquid and vapor phases becomes difficult with increasing number of trays, appearing that using conventional internals there is hardly any hope that distillation towers with many trays can be operated effectively in the cycling mode.¹³

Several solutions were suggested to solve the problem of the incomplete separation between the liquid and vapor flows, such as the use of external manifolds equalizing the pressure between trays at the beginning of each liquid-flow period¹⁴ or particular tray designs with inclined surfaces that introduced time delay in the liquid flow.¹⁵ However, a real breakthrough was only recently achieved when a new type of trays specially designed for cyclic operation mode was developed.^{3,6} The special trays are provided with valves and sluice chambers located under the trays—as shown in Figure 2.⁴ The operating principle is the following: during the vapor-flow period, the valves are in the up position and the liquid stays on the tray. During the liquid-flow period, the valves are in the down position and the liquid flows by gravity from the tray to the sluice chamber below the tray. When another vapor-flow period begins, the sluice chamber is opened and the liquid flows to the empty tray below. Using this type of tray, there are no complications related to the increased number of trays. Remarkable, MaletaCD has implemented already, in the food and petrochemical industry, cyclic distillation columns with 5 up to 42 trays, and column diameters of 0.4–1.7 m.

The development of cyclic distillation was also hampered by the fact that most simulation or design models of cyclic distillation were developed at a time when the available computing power was low and expensive. Consequently, the accuracy of the results was limited. The reported models

considered only binary mixtures and used drastic simplifying assumptions such as linear equilibrium, infinite reboiler, and negligible condenser holdup.^{11,12,14,16–20} These simplified assumptions were relaxed by recent studies that provided more realistic models.^{3,4} Also, noniterative design algorithms were only recently suggested and applied for mixtures with general nonlinear vapor–liquid equilibrium.^{4,7,21} In conclusion, there is a renewed interest in cyclic distillation due to the availability of design, control and simulation methods, and the introductions of specialized internals.

This article goes beyond simulations, being the first to describe experimental studies at pilot-scale for the operation of a stripping column equipped with specific trays⁶ and operated in cyclic mode, used industrially for concentrating ethanol. Moreover, it is the first study to validate experimentally the energy savings obtainable by cyclic distillation for an industrial beer column and to propose a new method for the determination of the mass-transfer efficiency of a cyclic distillation column based on the perfect displacement theoretical stage. The possible energy savings and separation efficiency are investigated and a comparison is made between simulation and experiments, while the underlying theory and modeling supporting the pilot-scale studies are also included.

Problem Statement

In spite of the major benefits promised by cyclic distillation (e.g., increased column throughput, lower energy requirements, and enhanced separation performance), the chemical process industry is still reluctant on the large scale implementation of this process intensification operation. The main reasons included the lack of design and control methods, as well as the perceived difficulty in operation due to the moving parts and alternating periods. Although the design and control methods as well as the process simulation were addressed by recent studies,^{4,7} the problem is that the experimental validation of improvements at industrial scale

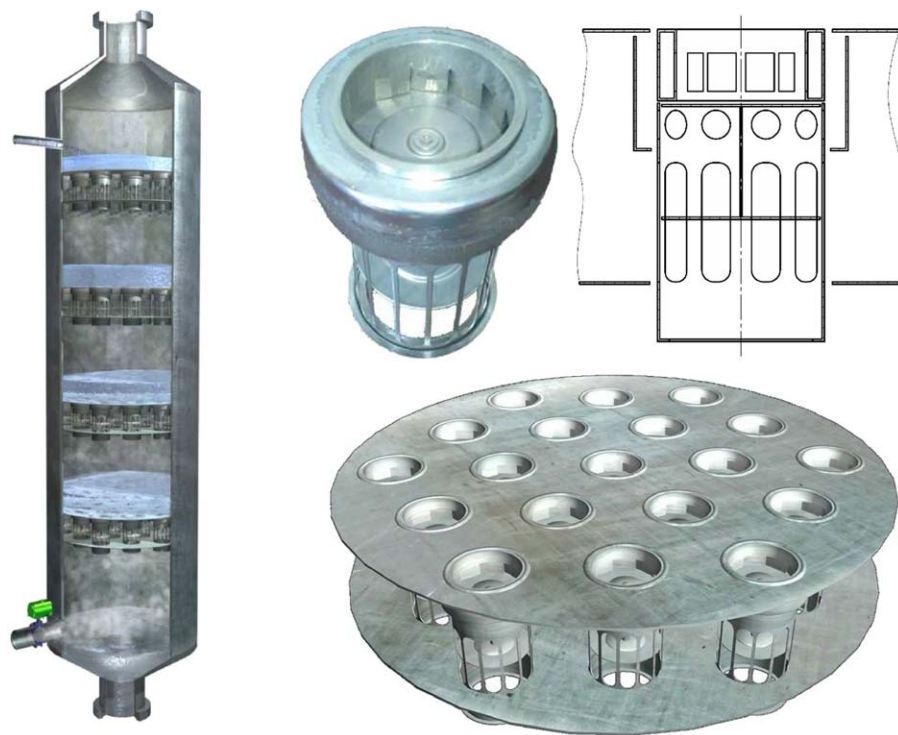


Figure 2. Cross-section of a cyclic distillation and specific internals (e.g., trays with sluce chambers).

[Color figure can be viewed in the online issue, which is available at wileyonlinelibrary.com.]

were so far not reported in literature. To address this issue, the goal of this study is to evaluate experimentally at pilot-scale, the operational and technological characteristic of a cyclic distillation column, and compare its separation efficiency with the existing beer column located at the State Enterprise Kosarsky Distillery Plant (UA).

Materials and Methods

This section describes the materials and methods used in the pilot-scale experimental study of a beer column operated in cyclic mode, in parallel to an existing beer column that was operated conventionally.

Experimental setup

A pilot-scale cyclic distillation column with a diameter of 310 mm, height 5500 mm was equipped with 10 Maleta trays,⁶ installed with a tray distance of 500 mm. The additional equipment used in the pilot plant includes: horizontal condenser (heat exchange area 10 m²), vertical condenser (heat exchange area 5 m²), hydro-seal (height 2500 mm), mash feed splitter, carbon dioxide separator, distillate tank (volume 0.4 m³), pump (1 m³/h), and pressure relief valves. The pilot-scale column was equipped with an automation system consisting of: PLC Schneider M340, frequency converter Schneider Altivar 12, pressure and temperature sensor Aplisens PC-28 and APC-2000 in top and bottom of the pilot column, flow sensor Krone H250, level sensor Aplisens APR-2200ALW-L, manual valves, and automatic Keystone K-LOK high performance butterfly valve. The thermal energy used in the pilot plant setup was supplied using an electric blanket. For convenience, Figure 3 plots the schematics of the pilot-scale cyclic distillation column.

The beer mash is fed at a temperature of 70–85 °C to a carbon dioxide separator (4) that removes CO₂ and other

gases. Afterwards, the stream is sent to a splitter (5) that divides the flow into two parts: one stream goes to the existing industrial column operated conventionally, and the second flow is used to feed the cyclic distillation column, via several valves (12, 13) and a flow meter (14). The cyclic operation mode is ensured by special mass-transfer devices and alternating the steam flow into the column through automatic valves (10, 11). Note that the maximum efficiency is possible in perfect displacement mode, when there is no mixing of the liquid on the adjacent trays during the overflow of liquid from one tray to the tray below. The basic idea of these special mass-transfer devices is to combine bubble trays with sluce chambers under each tray, thus being able to move of liquid from one tray to another without mixing of liquids from adjacent trays.

The top vapor outlet is fed to the condensers (2, 3), and the liquid distillate from the condensers goes through a flow meter (15) to the distillate tank (6), from which it is sent by a pump (16) to the hydro-selection column. In the distillate tank (6), the liquid level is maintained at 50%. Steam is fed to bottom of the column via several valves (10, 11, 18). The bottom product of the column goes through a hydro-seal (7) and removed as waste. Pressure relief systems (8, 9) are installed at the top and bottom of the column, to avoid any excess pressure. Note that a pseudo steady state is reached after about 70 operation cycles (equivalent to a period of about 0.5 h).

Measurement methods

The hydraulic resistance of the column was measured by differential pressure gauge Siemens SITRANS P DS III with a range of 0–150 kPa. The SITRANS P DS III series includes digital pressure transmitters for measuring gauge pressure, absolute pressure, differential pressure, flow, and level. The column is also setup with a viewing window that

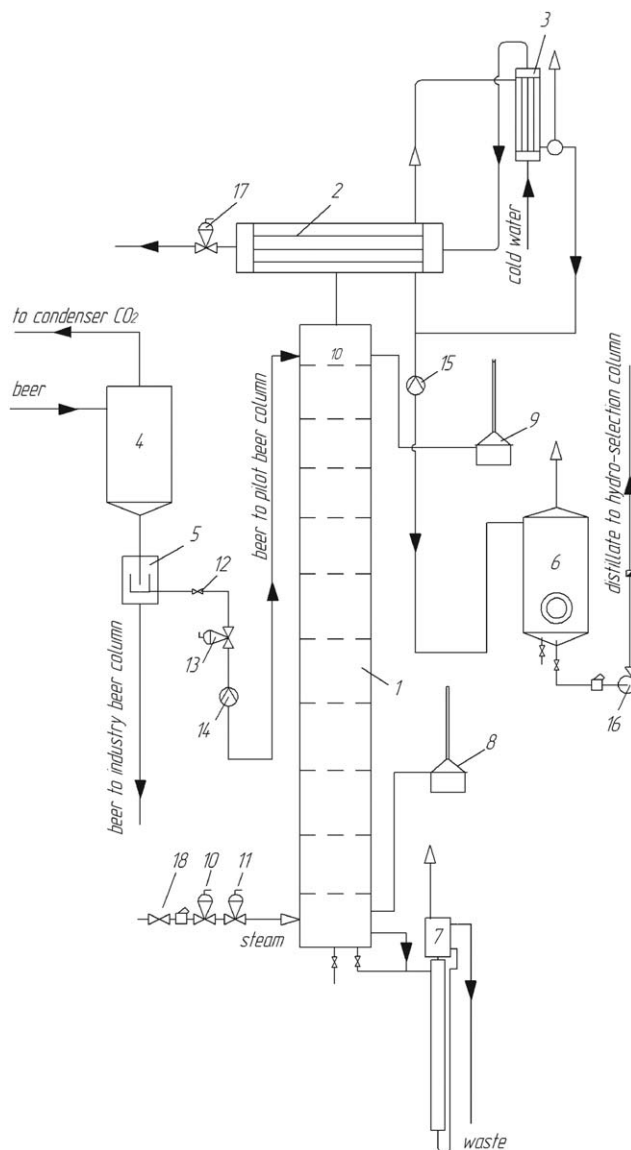


Figure 3. Schematics of the pilot-scale cyclic distillation column: 1—column shell, 2—main condenser; 3—auxiliary condenser, 4—carbon dioxide separator, 5—stream splitter, 6—distillate tank, 7—hydro-seal, 8, 9—pressure relief system, 10, 13, 17—analogue automatic valves, 14, 15—flow meters, 11—digital automatic valve, 12, 18—manual valves, and 16—distillate pump.

allows the visual inspection of the flow regime in the column. Flow meters Krohne H250 were used to measure the liquid flow rates. The temperature in top and bottom are measured with thermo-sensors Aplisens APC-2000 installed at appropriate places. A glass hydrometer was used for measurements of the ethanol concentration in the distillate stream. Analytical determinations were used to determine the concentration of ethanol in bottom product (waste), such as bio metric iodine chromatography method—which is based on titrimetric determination of the concentration of ethanol sodium thiosulfate, after the oxidation of ethanol to acetic acid using potassium dichromate in an acidic environment. The measurement error of the analysis is 0.1% vol in the feed line and distillate product and 0.002% vol in the waste

stream, respectively—based on the accuracy of the measurement methods. The consumption of steam in the pilot-scale cyclic distillation column was determined from the heat balance of the stripping column.

Experimental procedure

The experiments were performed during five days of continuous operation. The investigation of the column load was performed at liquid loads of $L = 8\text{--}24 \text{ m}^3/\text{m}^2\text{h}$ and steam load factor $F_s = 0.15\text{--}2.8$ (at a vapor velocity $V = 0.3\text{--}3.3 \text{ m/s}$). The height of the liquid layer on the tray was in the range of 50–100 mm. The duration of the operating cycle was changed within the range 12–40 s, and the duration of the liquid cycle (liquid transfer from tray to tray) was varied within 1–2 s. The pressure at the bottom of the column was kept within the range 108–111 kPa. An analog valve was usable to change the vapor supply, in case of pressure deviations.

The ethanol–water beer mixture (with an ethanol concentration of 9.0% vol) comes from the fermentation step using molasses as raw material and goes to the current beer conventional columns, as well as to the industrial pilot cyclic distillation column placed in parallel. The measured samples were obtained in the pilot cyclic distillation column from the stream splitter, distillate tank and bottom of column (waste), and for the classic column in the feed line, condenser, and bottom of column. The analysis was performed using the glass hydrometer for distillate and feed samples, and the bio metric iodine chromatography method for waste samples. The samples of feed and distillate were taken in a closed glass container, and the concentration of ethanol was determined using the glass hydrometer thermometer (0.10 °C point value using tables). The samples in the waste were taken from the bottom of the column in closed glass containers (100 mL), which were cooled and then the biometric iodine chromatography method was applied.

Mathematical model

The model of a tray column using separate phase movement consists of several equations³

1. Mass balance of the light key component (LKC), on the contact stage, during the vapor supply period

$$\frac{dx_n}{d\tau_v} = -\frac{G}{H}(y_n - y_{n-1}) \quad (1)$$

where n is the tray number, x_n is the molar fraction of LKC in the liquid on the tray n , y_n is the mol fraction of LKC in vapor leaving tray n , y_{n-1} is the molar fraction of LKC in vapor coming from tray $n-1$, H is the amount of liquid on the tray (mol), G is the gas (vapor) flow rate (mol/s), and τ_v is the vapor supply time (s).

2. Liquid flow hydrodynamics during the liquid period (liquid overflow from tray to tray)

$$x_n(0) = Fx_{n+1}(\tau_v) + (1-F)x_n(\tau_v) \quad (2)$$

where $F = H_1/H$ (with $0 < F \leq 1$) is the factor of liquid transfer delay, H_1 (mol) is the amount of liquid flowing from the tray, τ_v (s) is the vapor supply time.^{3,22}

3. Mass-transfer rate, determined by the local point efficiency (E_{OG}). Note that several type of efficiency have been used in distillation column modeling and design, including the overall, Murphree, Hausen, and vaporization efficiencies. Among them, the Murphree efficiency remains the most widely used by distillation engineers.

Table 1. Range of Operating Parameters Used for the Pilot-Scale Testing of the Cyclic Distillation Column

Parameter	Value Range	Parameter	Value Range
Consumption of steam (kg/L)	1.43–1.99	Pressure at bottom column (kPa)	108–111
Ethanol in feed (% vol)	9	Pressure at top column (kPa)	101–102
Ethanol in bottom (% vol)	0.015	Temperature at bottom column (°C)	101–102
Ethanol in distillate (% vol)	41.9–56.2	Temperature at top column (°C)	91–94
Feed flow rate mash (m ³ /hr)	0.9–1.2	Temperature of mash feed (°C)	85–90
Flow rate waste (m ³ /h)	0.9–1.2	Flow rate cooling water (m ³ /h)	2.0–3.5
Flow rate distillate (m ³ /h)	0.2–0.25		

$$E_{OG} = \frac{y_n(\tau_k) - y_{n-1}(\tau_k)}{y_n^*(\tau_k) - y_{n-1}(\tau_k)} \text{ where } \tau_k \in [0, \tau_v] \quad (3)$$

4. Equilibrium line (vapor composition as function of liquid composition)

$$y^* = f(x) \quad (4)$$

This system of equations can be also solved analytically, as showed by Robinson and Engel.²³ Thus, the concentration profiles on each stage can be described as follows

$$x_n(\tau) = e^{-\frac{G_m}{H}\tau} \sum_{i=1}^n C_i \frac{(\frac{G_m}{H}\tau)^{n-i}}{(n-i)!}; i = \overline{1, n} \quad (5)$$

with the boundary condition

$$x_i(0) = C_i \quad (6)$$

The simulation study of the pilot column and sensitivity analysis was carried using Mathworks Matlab R2012a. The modeling of the distillation process can be performed in both classic and cyclic mode. This is possible because the perfect displacement theoretical stage (cyclic mode) is turned into the perfect mixing theoretical stage (classic mode) when the liquid transfer delay approaches zero. The vapor–liquid equilibrium data of the ethanol–water system was used based on the non-random two-liquid (NRTL) property model. The adequacy of the simulated results was also checked with Aspen Plus (for the classical mode) and for the same output data, the same number of trays and concentration of LKC in bottom and top of column were determined. The following parameters were used for the simulations: liquid load 16.6 m³/m²h, column diameters 310 and 1600 mm, mash feed concentration 4–12% vol, steam usage 1.43–1.99 kg/L, and alcohol content in distillery dreg (waste) < 0.004% mol (or 0.015% vol). Note that the mass balance of the LKC is practically closed, at a level of 99.65%.

Results and Discussion

This section describes the results of the experimental work supported by sensitivity studies using simulations.

Experimental results

The pilot cyclic distillation column was tested under various conditions, within certain ranges for the operating parameters as described in Table 1. The value range of the parameters used in the pilot column is based on the industrial beer column conditions. A sensitivity analysis was performed by changing the feed flow rate of the mash stream, as well as the steam fed to the cyclic distillation column, while the other parameters (e.g., temperature, concentrations) are recorded as a result of the column operation—as described in Table 1.

The mash feed concentration was 9% vol ethanol in water. The pressure at the bottom of the column was kept at 109 kPa and above the top tray at 101 kPa. The temperature measured was within 85–90°C for the mash feed, 101–103°C for the distillery dreg, 53–55°C for distillate, and 91–92°C above the top tray. During the experimental tests, the liquid load was changed within $L = 14.3$ – 17.3 m³/m²h, while the vapor velocity ranged 0.7–0.94 m/s. The ratio liquid–vapor (L/G) was changed within the range 5.3–7.0. The specific steam usage per liter of absolute alcohol was within the range of 1.43–1.99 kg/L. The duration of vapor period was 38 s, and the liquid period was 2 s. The main results of experiments performed are given in Table 2. Note that the pilot-scale trials were performed in an industrial environment, so the range of experiments could not be extended beyond certain operational safety limits. However, the experiments performed cover a large range of operating conditions being sufficient for the aimed comparison of performance.

Depending on the liquid–vapor ratio, the alcohol concentration in the distillate stream was changed within 45–55% vol. To evaluate the possible range for the distillate concentration, the liquid–vapor ratio (L/G) was changed up to having alcohol concentrations in the distillery dreg (bottom product of beer column) as high as 0.007% vol. The content of alcohol in distillery dreg at low values of steam usage (1.43, 1.49, 1.51, and 1.61 kg/L) did not exceed the max value of 0.015% vol. The tests of the pilot-scale column confirmed the throughput capacity, and stability of operation was supported by the stable composition of the outlet streams.

Table 2. Operating Parameters for the Set of Pilot-Scale Experiments Performed

No.	V (m/s) Velocity	G _S (kg/L) Steam	G (kg/h) Steam	L (m ³ /m ² h) Liquid	Mash (% vol) Feed	X _B (% vol) Bottom	X _D (% vol) Distillate	L _F (kg/h) Feed	L _B (kg/h) Bottom	L _D (kg/h) Distillate
E1	0.89	1.89	184	14.4	9	0.008	43.21	1026	964	195
E2	0.94	1.99	193	14.3	9	0.007	41.9	1023	968	203
E3	0.80	1.54	165	15.9	9	0.015	56.7	1132	1071	193
E4	0.82	1.43	167	17.3	9	0.012	55.0	1166	1119	179
E5	0.87	1.61	180	16.6	9	0.011	53.4	1185	1025	188
E6	0.70	1.49	143	14.2	9	0.009	47.2	1011	971	196
E7	0.87	1.68	179	15.8	9	0.013	56.1	1124	1053	183
E8	0.81	1.51	167	16.4	9	0.008	55.8	1154	1064	180
E9	0.86	1.57	176	16.6	9	0.014	56.2	1185	1197	174

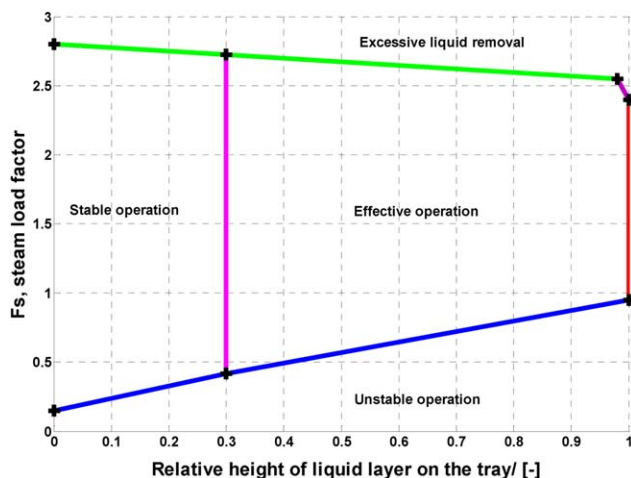


Figure 4. Operating ranges of the Maleta trays for various steam load factors and liquid heights on tray.

[Color figure can be viewed in the online issue, which is available at wileyonlinelibrary.com.]

A second study concerned the determination of the operating range for the Maleta trays, considering a relative liquid height per tray of h/h_{\max} where h is the actual height of the liquid layer on a tray and h_{\max} is the maximum possible height of the liquid layer on a tray. The liquid load was $L = 8\text{--}24 \text{ m}^3/\text{m}^2\text{h}$ and the steam load factor $F_s = 0.15\text{--}2.8$ (at a velocity of $V = 0.3\text{--}3.3 \text{ m/s}$). Note that the steam load factor is defined as

$$F_s = V\sqrt{\rho_G} \frac{m}{s} \left(\frac{\text{kg}}{\text{m}^3} \right)^{1/2} \quad (7)$$

where F_s is the steam load factor, ρ_G is the gas (vapor) density (kg/m^3), and V is the vapor velocity (m/s).

Figure 4 shows the operating ranges of the Maleta trays for various steam load factors and liquid heights on tray. The dependency is linear, such that with an increased amount of liquid on the tray, the steam flow rate has to be increased. The operating range of the column is limited below by an unstable operation region, in the top by and excessive liquid removal, on the right by excessive liquid flow. Note that insufficient liquid on tray leads to a lack of stable bubbling and reduced efficiency of the column due to the mixing of the liquid from adjacent trays. The effective operation range of the column is characterized by a uniform mode and intense bubbling on a tray.

Analysis of pilot-scale cyclic distillation and classic industrial columns

The pilot-scale cyclic distillation column has 10 trays of 310 mm diameter, while the existing classic industrial beer column has 26 sieve trays with a diameter of 1600 mm—details given in Table 3. Remarkable, for the same performance, the number of trays needed for the cyclic distillation operation is 2.6 times lower as compared with the classic industrial column, while a reduction of steam usage of 0.4–0.6 kg/L (17–30%) was also possible.

Note that the periodic operation mode does not add any control difficulties. Indeed, similarly to conventional distillation, the amount of distillate and bottoms withdrawn from the column controls the level in the reflux drum and reboiler.

For quality control, one can measure temperatures in the stripping and rectifying section at certain moments in time, for example, at the end of the vapor-flow period. Then, by means of a suitable discrete-time control algorithm, the rate of vapor flow or the duration of the next vapor-flow period are adjusted. In this way, feed rate and composition disturbances are effectively rejected.⁴

Figure 5 illustrates the pressure and temperature profiles measured during the cyclic operation of the pilot-scale column. The pseudo steady-state data confirms the stable operation of the column. During the vapor period, a deviation of maximum 3% from the set point pressure of 12 kPa is encountered. When the steam feed stops (during the liquid period), the pressure in bottom of the column decrease from 12 to 6 kPa, but as no vapor-liquid contact exists during this period, the column operation is not affected. Note that the concentrations were measured by sampling, so no continuous recordings are available. Nonetheless, the concentration is directly dependent on the measured temperature and pressure, which are already presented in Figure 5.

Energy savings in cyclic distillation

Based on theoretical concepts of cyclic and classic distillation, one can make use of a graphical interpretation to evaluate the potential energy savings. Let us consider a column with three trays (Figure 6). The amount of ethanol that enters the column is Lx_p (mol/h), and the amount of ethanol in the bottom product is Lx_0 (mol/h). The amount of ethanol that is supplied to column with vapor is Gy_0 (mol/h) and the amount of ethanol that comes out is Gy (mol/h). Figure 6 shows the process operating lines for classic distillation and cyclic operating modes. Considering an equal number of trays and same LKC content at the bottom of the column, the mass balance is

$$L(x_p - x_0) = G_1y_1; L(x_p - x_0) = G_2y_2 \quad (8)$$

According to the classic theoretical stage model, the LKC concentration on the first top tray will be x_1 and it is not changed in time. The equilibrium value of LKC in vapor phase is y_1 . Hence, the average value of LKC concentration in the vapor leaving the tray and the local value are equal (Figure 6a). However, in the cyclic operation mode, the LKC concentration on the tray is variable during the vapor

Table 3. Operating Parameters for the Cyclic Distillation and Classic Industrial Columns

Parameter	Classic Industrial Column	Pilot-Scale Cyclic Distillation Column
Column diameter (mm)	1,600	310
Height of the column (mm)	13,000	5,500
Number of trays (–)	26	10
Liquid flow rate ($\text{m}^3/\text{m}^2\text{h}$)	12–15	14.3–17.3
Vapor velocity (m/s)	0.6–1.2	0.7–0.94
Steam usage (kg/L)	2.0–2.4	1.43–1.99
Feed composition (% vol ethanol)	9.0	9.0
Distillate composition (% vol ethanol)	40–45	41.9–56.2
Bottoms composition (% vol ethanol)	0.015	0.015
Feed temperature ($^{\circ}\text{C}$)	85–90	85–90
Feed tray temperature ($^{\circ}\text{C}$)	93–94	91–92
Bottom temperature ($^{\circ}\text{C}$)	102–105	101–103
Top pressure (kPa)	102–103	101–102
Bottom pressure (kPa)	116–120	108–111

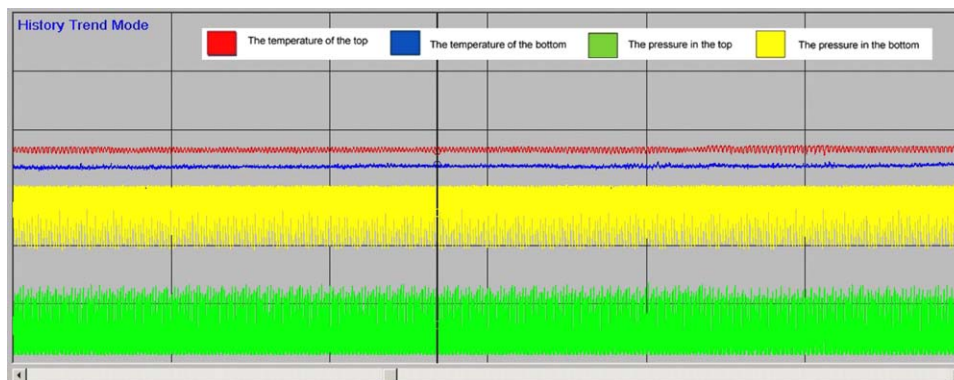


Figure 5. Temperature and pressure historian trends for the cyclic distillation column.

[Color figure can be viewed in the online issue, which is available at wileyonlinelibrary.com.]

period for each point in time, so the average value of the LKC concentration in vapor (y_2) during vapor period is used (Figure 6b). Note that the LKC average concentration in vapor phase for cyclic operation mode (y_2) is higher than for the classic mode (y_1). As the column mass balance for LKC is preserved ($Gy_1 = Gy_2$), the vapor flow rate required for the separation in cyclic mode is lower ($G_2 < G_1$) as the LKC concentration in vapor is higher ($y_2 > y_1$). Thus, the revamping of classic distillation columns into cyclic mode results in major energy savings, proportional with $\Delta y = y_2 - y_1$. Remarkable, in case of the pilot-scale cyclic distillation beer column, the determined energy saving in terms of steam usage are 0.4–0.6 kg/L, amounting 17–30% saving as compared with the classic distillation column—and notably using 2.6 times fewer stages (10 instead of 26).

It worth noting that the revamping of classic distillation columns for cyclic operation mode can be done by simple changing the distillation trays with Maleta trays, and add one vapor control valve for the steam fed to the bottom of the column. These trays can work in dual-mode (cyclic and conventional), but in the conventional operating regime, all the advantages of cyclic distillation are lost. Note that in case of conventional operation (continuous flow of vapor and liquid), the valve of the mass-transfer device rises and falls erratically during the continuous feed of vapor—while the liquid continuously flows down the column similar to classic trays.

Sensitivity analysis

The sensitivity analysis was performed by simulating the pilot-scale cyclic distillation column (experiment E5 in Table 2): liquid flow rate 16.6 m³/m²h, column diameter 310 mm, mash feed concentration 9% vol, steam usage over 1.6 kg/L, and ethanol in distillery dreg <0.004% mol (or 0.015% vol). Three cases were simulated and compared for the experiment E5: (1) perfect displacement model (cyclic distillation, $E_{OG} = 1$ and $F = 1$) with 6 theoretical trays; (2) perfect mixing model (classic distillation, $E_{OG} = 1$ and $F = 0.05$) with 16 trays; and (3) pilot-scale cyclic distillation column with 10 trays ($E_{OG} = 0.78$ and $F = 0.92$). Accordingly, the operating lines and concentration profiles are plotted in Figures 7–9, respectively.

The shape and position of operating lines show the advantages of the perfect displacement model (cyclic distillation) as compared with the perfect mixing model (classic distillation). The average Murfree efficiency of the trays is 285% in first case, 100% in second case, and 145% in the third case, respectively. The local efficiency for the pilot-scale cyclic distillation column is $E_{OG} = 0.78$, and the F factor is 0.92. A tray efficiency exceeding 100% is due to the fact that in the perfect displacement model, the average value of concentration changes in LKC is larger than the value corresponding to the equilibrium with the fluid leaving the tray in the perfect mixing model. For this reason, even with a local efficiency of 0.78, the pilot-scale cyclic distillation column has

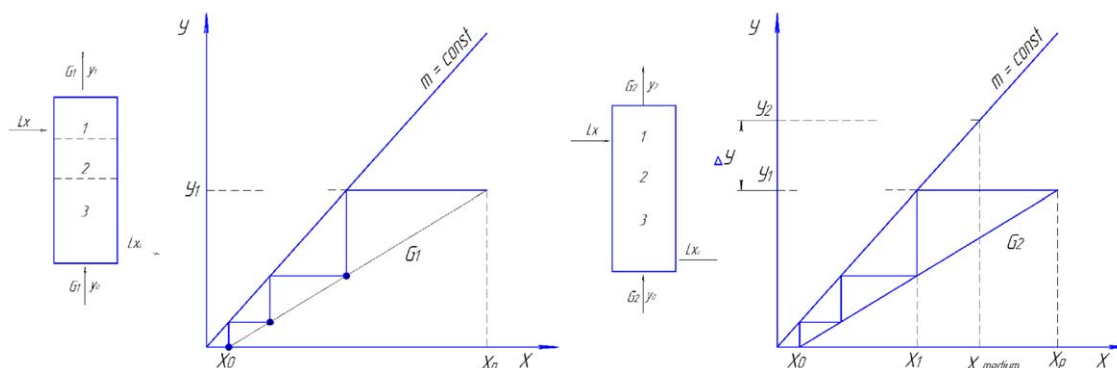


Figure 6. Operating line and material balance of the distillation column: (a) cyclic operation mode and (b) classic operation, where x_p is the feed composition, x_{cp} average concentration in liquid (cyclic distillation), x_1 is the concentration of LKC in liquid (classic distillation), y_2 is the average concentration of LKC in vapor (cyclic distillation), and y_1 is the concentration of LKC in vapor (classic distillation).

[Color figure can be viewed in the online issue, which is available at wileyonlinelibrary.com.]

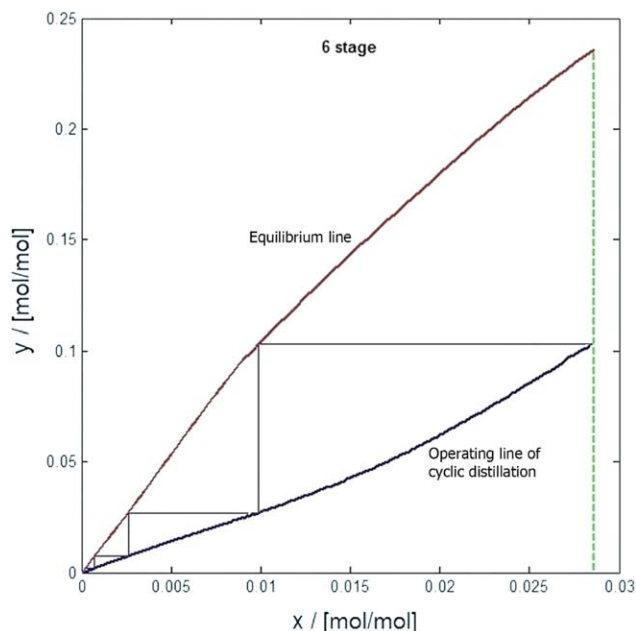


Figure 7. Operating lines of cyclic distillation using the perfect displacement theoretical stage (six stages).

[Color figure can be viewed in the online issue, which is available at wileyonlinelibrary.com.]

a tray efficiency of over 100% (as compared with the perfect mixing model). Figure 10 shows the distribution of Murfree efficiency along the trays in the three simulated cases. The maximum efficiency of the process in pilot column is observed at trays 6–8. This phenomenon is due to the diffusion potential varying with the location.

Another sensitivity analysis was performed to evaluate the steam usage in the ethanol production for mash feed concen-

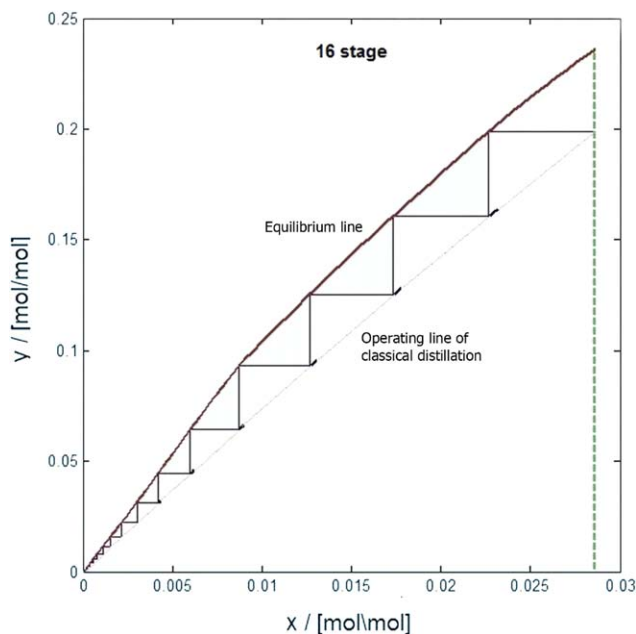


Figure 8. Operating lines of classical distillation using the perfect mixing theoretical stage (16 stages).

[Color figure can be viewed in the online issue, which is available at wileyonlinelibrary.com.]

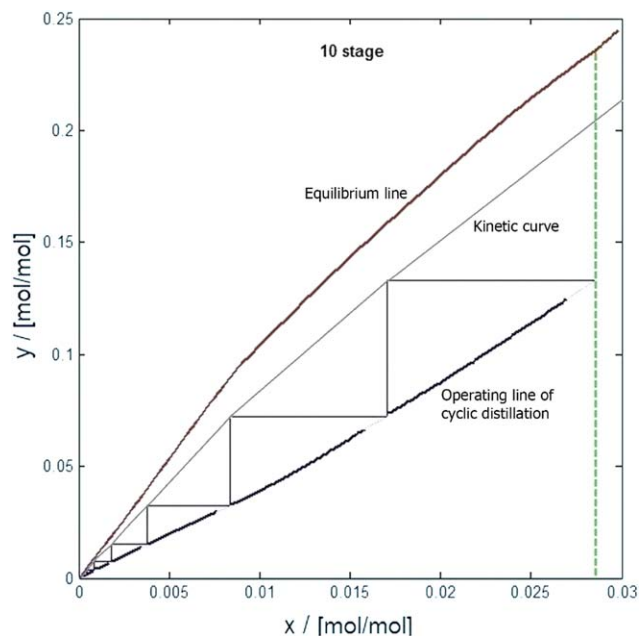


Figure 9. Operating lines of cyclic distillation (pilot-scale column) using perfect displacement (10 stages), where the kinetic curve refers to the mass-transfer limited pseudo-equilibrium line.

[Color figure can be viewed in the online issue, which is available at wileyonlinelibrary.com.]

trations of 4–12% vol. The pilot-scale distillation column (10 trays with a diameter of 310 mm) was considered with perfect displacement and perfect mixing, respectively. The liquid flow rate is $17.3 \text{ m}^3/\text{m}^2\text{h}$. Figure 11 illustrates that for perfect displacement (cyclic distillation), the steam usage is significantly lower as compared with the perfect mixing (classic distillation). For a mash feed concentration of 10% vol, the steam usage is 1.2 kg/L for perfect displacement and 1.7 kg/L for perfect mixing, while for a mash feed concentration of 4% vol, the steam usage is 2.8 kg/L (perfect displacement) and 4.0 kg/L (perfect mixing). The experimental measurements indicate that the pilot-scale cyclic distillation

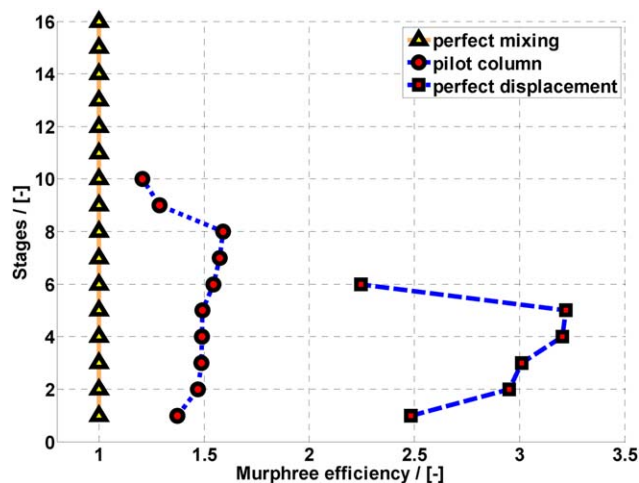


Figure 10. Variation of the Murphree efficiency with the stage number (column location).

[Color figure can be viewed in the online issue, which is available at wileyonlinelibrary.com.]

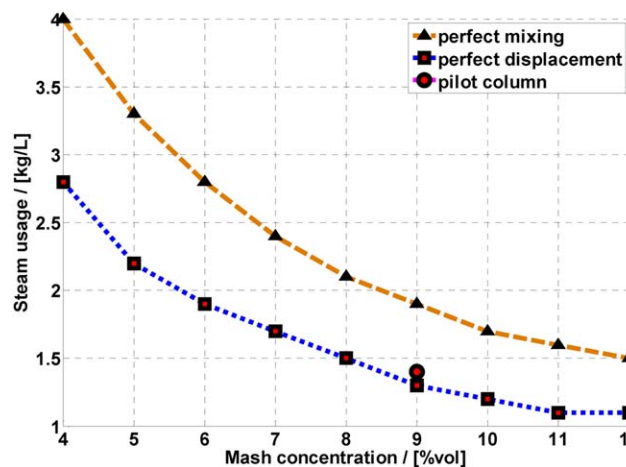


Figure 11. Dependence between steam consumption and the number of theoretical trays.

[Color figure can be viewed in the online issue, which is available at wileyonlinelibrary.com.]

column is operated close to the perfect displacement mode, having a steam usage that is 1.4 times lower as compared with the classic distillation column.

It is worth noting that the steam usage values are similar to the recent literature reports (values given as kilogram steam per kilogram ethanol produced): 2.5 (classic distillation), 1.18 (heat-integrated distillation), 1.17 (very high gravity), and 1.13 (pervaporation).²⁴

The last sensitivity analysis addressed the number of theoretical stages required for the classic and the cyclic distillation systems, considering a mash feed concentration range of 4–12% vol and a steam usage of 1.4–2.0 kg/L. Table 4 provides an overview of the simulation results. In all cases, when the steam usage is decreased, the number of trays required for the same separation performance increases. Furthermore, the same number of trays can provide a specific separation performance at different steam usage rates and mash feed concentrations. Notably, this range is wider for the cyclic distillation that uses a significantly lower number of theoretical trays as compared with the classic distillation. Figure 12 shows a comparison between the simulation and experimental results—in terms of number of stages required vs. steam usage—for the pilot cyclic distillation column and the classic industrial beer column. For the cyclic distillation, there is clearly a good match between the simulated conditions and the experimental results in the pilot column. Considering ten trays, the pilot column uses slightly more steam

Table 4. Numbers of Theoretical Stages Required at Various Steam Usage and Different Mash Feed Concentrations

	Steam use (kg/L)	Mash Feed Concentration (% vol)									
		4	5	6	7	8	9	10	11	12	
Classic distillation	1.4	—	—	—	—	—	—	—	13	11	
	1.6	—	—	—	—	—	16	12	10	9	
	1.8	—	—	—	—	15	11	10	8	8	
	2.0	—	—	—	16	11	9	8	8	7	
Cyclic distillation	1.4	—	—	—	—	13	8	7	6	5	
	1.6	—	—	—	12	8	6	4	4	4	
	1.8	—	—	13	8	6	5	4	4	4	
	2.0	—	16	9	6	5	4	4	3	3	

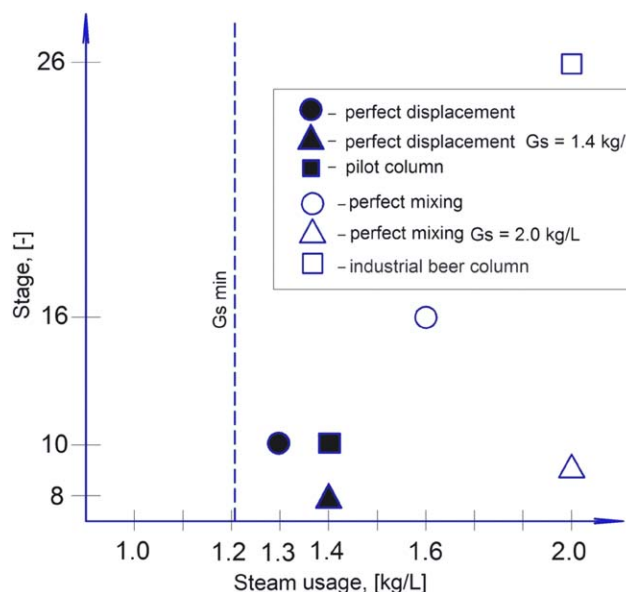


Figure 12. Comparison between the simulation and experimental results—in terms of number of stages required vs. steam usage—for the pilot cyclic distillation column and the classic industrial beer column.

[Color figure can be viewed in the online issue, which is available at wileyonlinelibrary.com.]

(0.1 kg/L) as compared with the ideal simulated case. Alternatively, for the same steam usage of 1.4 kg/L, the pilot column needs 10 trays, as compared with eight trays required in the simulated ideal case. A similar comparison can be made for the classic distillation, but here, the differences are larger due to the lower stage efficiency as compared with a simulated ideal classic tray.

Figure 13 illustrates the efficiency of the pilot-scale cyclic distillation column expressed according to the perfect mixing and perfect displacement model, respectively. Input data for calculation is taken from Table 2. The column efficiency

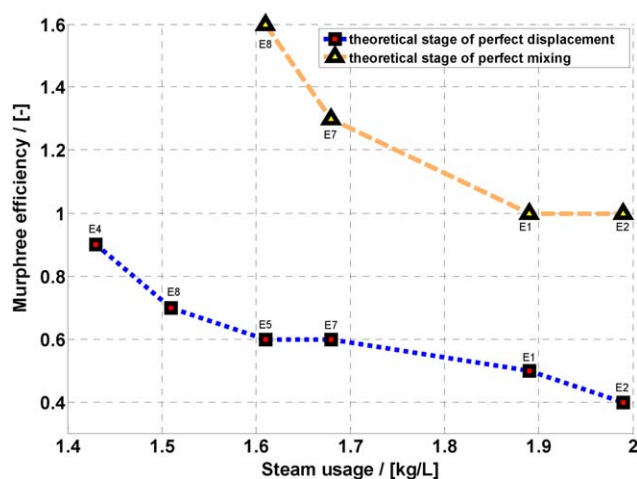


Figure 13. Efficiency of the pilot-scale cyclic distillation column expressed according to the perfect mixing and perfect displacement model, respectively.

[Color figure can be viewed in the online issue, which is available at wileyonlinelibrary.com.]

calculated according to the perfect mixing theoretical stage is in the range of 100–160%. When the column efficiency is calculated according to the perfect displacement theoretical stage, the range is 40–90%. Note that the efficiency of a column operated in a cyclic mode should be also calculated based on the perfect displacement theoretical stage, to avoid reporting only conventional efficiencies of over 100% that might be misleading to readers.

It is worth mentioning that the mass-transfer efficiency does not depend on the column diameter, but depends on the liquid-vapor ratio (L/G) in the column—although the height of the liquid layer on the trays should be similar for different tray diameters, to provide the same mass-transfer rate on trays with different diameters. During the vapor period (when the mass transfer takes place), the liquid stays on the trays so it is not leaking—this means that the trays can have any geometric shape as the liquid overflow takes place only in the vertical plane. In practical operation, no problems were observed in the plug-flow behavior in columns of 300–3000 mm diameter.

Conclusions

Cyclic distillation can bring new life to old distillation columns, by simply changing the internals and operating mode, and therefore, providing key benefits, such as: increased column throughput, lower energy requirements as well as better separation performance. The simulation and experimental studies of a pilot-scale cyclic distillation beer column used for concentrating ethanol, confirmed the theoretical expectations, leading to the following key results and conclusions:

- Higher throughput and equipment productivity is possible, as compared with conventional distillation. Increasing the liquid load (15–17.3 m³/m²h) does not lead to an increase in the hydraulic resistance and flooding, as the amount of liquid on a tray remains constant, and only the cycle frequency is changed and consequently, the residence time of the liquid on trays is decreased.
- Reduced energy requirements, such that a required purity can be achieved with lower vapor flow rates, at the same number of trays. In case of a beer mash feed concentration of 4–12% vol, cyclic distillation has a steam usage of about 1.4 times less (~30%), while using 2.6 times fewer trays as compared with the classic distillation column.
- The maximum efficiency of the process corresponds to the minimum steam consumption. This result is due to the fact that in theoretical calculations, increasing the steam flow rate leads to fewer trays. However, in the pilot-scale experiments, the number of trays in the column is fixed, so the real effectiveness of the trays will decrease, with increasing the steam flow rate.
- High tray efficiencies are possible, such that at same vapor flow rate, a required purity can be obtained using fewer trays—which allows for reduced capital costs. The efficiency of the pilot-scale cyclic distillation column was 100–160% according to the perfect mixing theoretical stage model (classic distillation), or 40–90% according to the perfect displacement theoretical stage model. The latter way of reporting should be used to remove any potential confusion when comparing classic to cyclic mode.

Considering the benefits of cyclic operation over classic distillation, other potential applications are envisaged, such

as: biofuels production (e.g., bioethanol, biobutanol, biodiesel), organic synthesis, specialty chemicals, gas processing, petrochemicals, and pharmaceuticals.

Acknowledgment

The authors would like to thank Professor Vitaliy Taran (National University of Food Technologies, Ukraine) for the open prospects of cyclic distillation and developing together this research area for industrial use.

Notation

E_0 = local efficiency (–)
 F = liquid delay factor (–)
 F_s = steam load factor, m/s (kg/m³)^{1/2}
 G = vapor flow rate, mol/s
 G_s = steam usage, kg/L
 H = holdup of liquid on tray, mol
 L = liquid load, m³/m²h
 LKC = light key component
 m = mass, kg
 n = number of theoretical trays (–)
 t = time, s
 V = vapor velocity, m/s

Greek symbols

λ = diffusion potential factor (–)
 τ_v = vapor-flow period, s
 τ_L = liquid-flow period, s
 τ_C = total cycle time, s

Literature Cited

1. Kiss AA. *Advanced Distillation Technologies—Design, Control and Applications*. Chichester, UK: Wiley, 2013.
2. Kiss AA, Flores Landaeta SJ, Infante Ferreira CA. Towards energy efficient distillation technologies—making the right choice. *Energy*. 2012;47:531–542.
3. Maleta VN, Kiss AA, Taran VM, Maleta BV. Understanding process intensification in cyclic distillation systems. *Chem Eng Process*. 2011;50:655–664.
4. Patrut C, Bildea CS, Lita I, Kiss AA. Cyclic distillation—design, control and applications. *Sep Purif Technol*. 2014;125:326–336.
5. Cannon MR. Controlled cycling improves various processes. *Ind Eng Chem*. 1961;53:629–629.
6. Maleta B, Maleta O. Mass exchange contact device. US Patent 8,158,073, 2012.
7. Patrut C, Bildea CS, Kiss AA. Catalytic cyclic distillation—a novel process intensification approach in reactive separations. *Chem Eng Process*. 2014;81:1–12.
8. Gaska RA, Cannon MR. Controlled cycling distillation in sieve and screen plate towers. *Ind Eng Chem*. 1961;53:630–631.
9. McWhirter JR, Cannon MR. Controlled cycling distillation. *Ind Eng Chem*. 1961;53:632–634.
10. Schrodt VN, Sommerfeld JT, Martin OR, Parisot PE, Chien HH. Plant-scale study of controlled cyclic distillation. *Chem Eng Sci*. 1967;22:759–767.
11. Matsubara M, Watanabe N, Kurimoto H. Binary periodic distillation scheme with enhanced energy conservation I—principle and computer simulation. *Chem Eng Sci*. 1985;40:715–721.
12. Matsubara M, Watanabe N, Kurimoto H, Shimizu K. Binary periodic distillation scheme with enhanced energy conservation II—experiment. *Chem Eng Sci*. 1985;40:755–758.
13. Larsen J, Kümmel M. Hydrodynamic model for controlled cycling in tray columns. *Chem Eng Sci*. 1979;34:455–462.
14. Furzer IA. Mass transfer in a periodically cycled plate column fitted with a manifold. *Chem Eng Sci*. 1980;35:1299–1305.
15. Szonyi L, Furzer IA. Periodic cycling of distillation-columns using a new tray design. *AIChE J*. 1985;31:1707–1713.
16. Sommerfeld JT, Schrodt VN, Parisot PE, Chien HH. Studies of controlled cyclic distillation: I. Computer simulations and the analogy with conventional operation. *Sep Sci Technol*. 1966;1:245–279.

17. Rivas OR. An analytical solution of cyclic mass transfer operations. *Ind Eng Chem*. 1977;16:400–405.
18. Duffy GJ, Furzer IA. Periodic cycling of plate columns: analytical solution. *Chem Eng Sci*. 1978;33:897–904.
19. Baron G, Wajc S, Lavie R. Stepwise periodic distillation—I: total reflux operation. *Chem Eng Sci*. 1980;35:859–865.
20. Baron G, Wajc S, Lavie R. Stepwise periodic distillation—II: separation of a binary mixture. *Chem Eng Sci*. 1981;36:1819–1827.
21. Toftegard B, Jorgensen SB. Design algorithm for periodic cycled binary distillation columns. *Ind Eng Chem Res*. 1987;26:1041–1043.
22. Maleta VN, Maleta BV. Hydrodynamics of liquid flow in the model of theoretical stage with perfect displacement. *J Chem Chem Eng*. 2011;5:25–29.
23. Robinson RG, Engel AJ. Analysis of controlled cycling mass transfer operations. *Ind Eng Chem*. 1967;59:22–29.
24. Baeyens J, Kang Q, Appels L, Dewil R, Lv Y, Tan T. Challenges and opportunities in improving the production of bio-ethanol. *Prog Energy Combust Sci*. 2015;47:60–88.

Manuscript received Feb. 20, 2015, and revision received Mar. 30, 2015.